May 2005, Vol.20, No.3, pp.411–418 J. Comput. Sci. & Technol.

Wavelet Energy Feature Extraction and Matching for Palmprint Recognition

Xiang-Qian Wu[1], Kuan-Quan Wang[1], and David Zhang[2]

[1] *School of Computer Science and Technology, Harbin Institute of Technology, Harbin 150001, P.R. China*

[2] *Biometrics Research Centre, Department of Computing, Hong Kong Polytechnic University Hong Kong Special Administrative Region, P.R. China*

E-mail: xqwu@hit.edu.cn; wangkq@hit.edu.cn; csdzhang@comp.polyu.edu.hk

Received December 10, 2003; revised August 10, 2004.

Abstract According to the fact that the basic features of a palmprint, including principal lines, wrinkles and ridges, have different resolutions, in this paper we analyze palmprints using a multi-resolution method and define a novel palmprint feature, which called wavelet energy feature (WEF), based on the wavelet transform. WEF can reflect the wavelet energy distribution of the principal lines, wrinkles and ridges in different directions at different resolutions (scales), thus it can efficiently characterize palmprints. This paper also analyses the discriminabilities of each level WEF and, according to these discriminabilities, chooses a suitable weight for each level to compute the weighted city block distance for recognition. The experimental results show that the order of the discriminabilities of each level WEF, from strong to weak, is the 4th, 3rd, 5th, 2nd and 1st level. It also shows that WEF is robust to some extent in rotation and translation of the images. Accuracies of 99.24% and 99.45% have been obtained in palmprint verification and palmprint identification, respectively. These results demonstrate the power of the proposed approach.

Keywords biometrics, palmprint recognition, wavelet energy feature, weighted city block distance

1 Introduction

As computer-aided identity recognition becomes increasingly important, biometrics is taking its place as one of the most secure, flexible and reliable of the available approaches[1,2]. The most widely used biometric feature is the fingerprint[3,4] while the most reliable one is the iris[5,6]. However, it is very difficult to extract small unique features (known as minutiae) from unclear fingerprints[3,4] and the iris input devices are very expensive. Other biometric features, such as face[7,8] and voice[9,10], are less accurate and they can be mimicked easily. The palmprint, as a relatively new biometric feature, has several advantages compared with other currently available features[11]: palmprints contain more information than fingerprint, so they are more distinctive; palmprint capture devices are much cheaper than iris devices; palmprints also contain additional distinctive features such as principal lines and wrinkles, which can be extracted from low-resolution images; a highly accurate biometrics system can be built by combining all features of palms, such as palm geometry, ridge and valley features, and principal lines and wrinkles, etc.

A palmprint has three types of basic features: principal lines, wrinkles, and ridges (see Fig.1) and they have been analysed in various ways. Zhang[12] and Duta[13] employed palm lines, including principal lines and wrinkles, for identity recognition. Li[14] analysed them in the frequency domain. Zhang[1] also identified individuals by extracting texture features, which were constituted by these basic features, from palmprints. You[15] proposed a hierarchical method of palmprint identification based on global textural feature and interesting points. Han[16] used the operator-based approach to extract the line-like features from palmprints for palmprint verification. In all of these methods, palmprints were analysed in a single resolution. However, these basic features in palmprints have intrinsic multi-resolution characters: the principal lines are the thickest, so they can be analyzed in low resolutions; the wrinkles are thinner than the principal lines and can be analyzed in medium resolutions and the ridges are the thinnest, thus they should be analyzed in high resolutions. Therefore, it is very suitable to analyze palmprints using multi-resolution methods.

Wavelets[17−19] are powerful tools of multi-resolution analysis, which have been used widely in biometrics based identity recognition systems[6]. A two-dimensional wavelet transform can decompose the image in several directions at different resolutions (scale), which is very advantageous to characterize palmprints since their basic features have different directions and different resolutions. Moreover, to a nonoscillating pattern, the amplitudes of wavelet coefficients increase when the scale of wavelet decomposition increase, whereas, to a high frequency oscillating pattern, the amplitudes of wavelet coefficients at large scales are much smaller than at fine scale which matches the spatial frequency of the oscillations[18]. In a palmprint, the principal lines and wrinkles are nonoscillating patterns while the ridges are oscillating pattern. As a result, the distributions of their wavelet energy, in this paper defined

*Short Paper

Supported by the National Natural Science Foundation of China under Grant No.60441005.

by using wavelet coefficients, are different at each scale of wavelet decomposition. Therefore, wavelet energy is well suited to describing a palmprint. Wavelet energies of different decomposition levels have different powers to discriminate palmprints. Thus, when matching palmprints, we choose a suitable weight for each level to compute a weighted cityblock distance according to the discriminability of this level WEF.

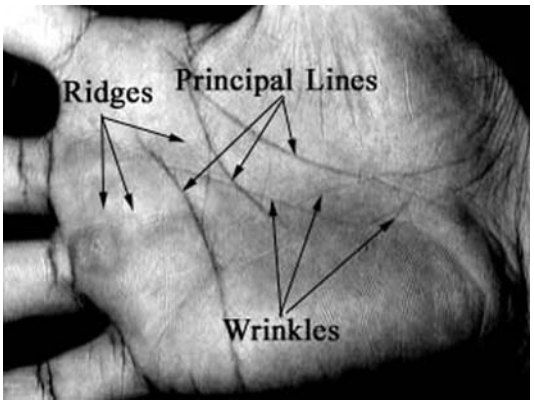

Fig.1. Three types of basic features in a palmprint.

The paper is organized as follows. Section 2 provides a palmprint preprocessing technique. Section 3 describes the wavelet energy feature construction and matching in detail. Section 4 provides experimental results and comparisons, and Section 5 gives a conclusion.

2 Palmprint Preprocessing

When palmprints are captured, the position and direction of a palm may vary so that even palmprints from the same palm may have a little rotation and translation. Furthermore, palms differ in size. Hence palmprint images should be orientated and normalized before feature extraction and matching. In our CCD-based palmprint capture device[13], there are some pegs between fingers to limit the palm's stretching, translation and rotation (Fig.2(a)). These pegs separate the fingers, which enables us to use the points on the fingers' boundary to align and normalize palmprints. An original palmprint captured by the device is shown in Fig.2(b). There are six main steps in the preprocessing.

Step 1. Smooth the original image by a low-pass filter and use a threshold to convert it to a binary image (see Fig.2(c)).

Step 2. Trace the palm's boundary (see Fig.2(d)).

Step 3. Use straight lines (L^1, L^2, L^3, and L^4) to fit the segments of the boundary of the first finger, middle finger, third finger and little finger (see Fig.2(e)):

$$L^i : y = k_i x + b_i \tag{1}$$

where k_i and b_i are the slope and intercept of L^i ($i = 1, \ldots, 4$), which can be computed by the following equations:

$$k_i = \frac{\sum_{k=1}^{M_i} x_i^k \times \sum_{k=1}^{M_i} y_i^k - M_i \times \sum_{k=1}^{M_i} (x_i^k \times y_i^k)}{\left(\sum_{k=1}^{M_i} x_i^k\right)^2 - M_i \times \sum_{k=1}^{M_i} (x_i^k)^2} \tag{2}$$

$$b_i = \frac{\sum_{k=1}^{M_i} y_i^k - k_i \times \sum_{k=1}^{M_i} x_i^k}{M_i} \tag{3}$$

where $\{(x_i^k, y_i^k)\}_{k=1}^{M_i}$, $(i = 1, \ldots, 4)$ are the coordinates of the points on the segments of the boundary of the first finger, middle finger, third finger and little finger,

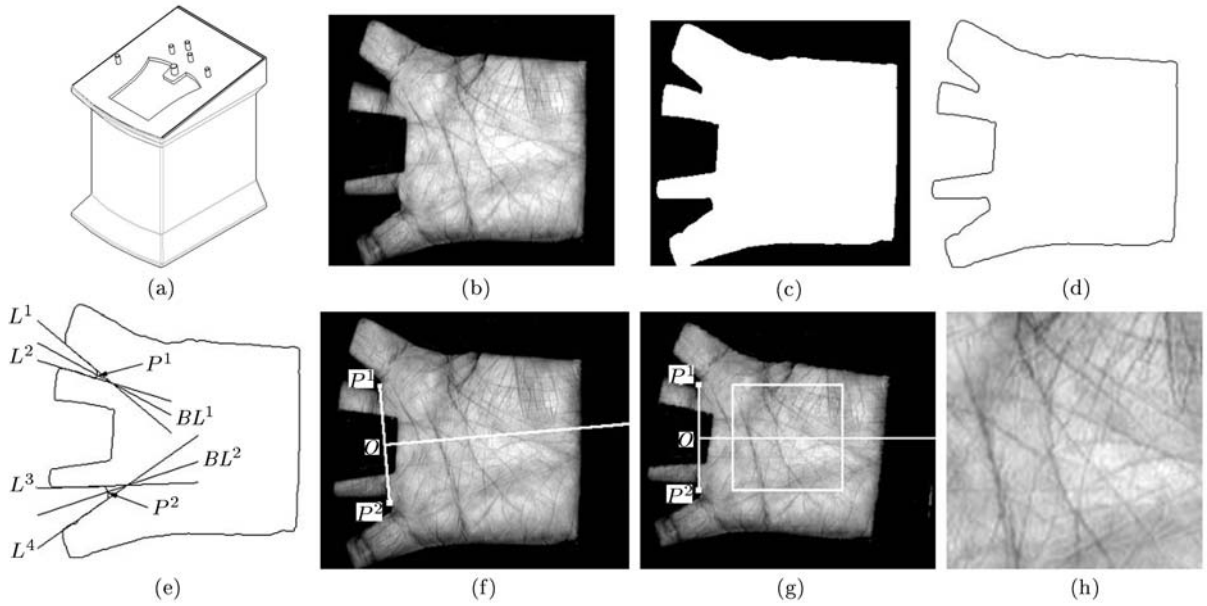

Fig.2. Main steps of preprocessing. (a) Palmprint capture device. (b) Original image. (c) Binary image. (d) Boundary tracking. (e) Line fitting, bisectors and intersections. (f) Palmprint coordinate system. (g) Central part extraction. (h) Preprocessed result.

respectively; M_i is the total number of the points on the corresponding segment.

Step 4. Computing the bisectors (BL^1 and BL^2) of the angles formed by L^1 and L^2, L^3, and L^4:

$$BL^i : y = K_i x + B_i \tag{4}$$

where K_i and B_i are the slope and intercept of BL^i ($i = 1, 2$), which can be computed by the following equations:

$$K_i = \frac{k_{2\times i-1} \times \sqrt{1 + k_{2\times i}^2} + k_{2\times i} \times \sqrt{1 + k_{2\times i-1}^2}}{\sqrt{1 + k_{2\times i-1}^2} + \sqrt{1 + k_{2\times i}^2}} \tag{5}$$

$$B_i = \frac{b_{2\times i-1} \times \sqrt{1 + k_{2\times i}^2} + b_{2\times i} \times \sqrt{1 + k_{2\times i-1}^2}}{\sqrt{1 + k_{2\times i-1}^2} + \sqrt{1 + k_{2\times i}^2}} \tag{6}$$

where $i = 1, 2$; $k_1 \sim k_4$, $b_1 \sim b_4$ are computed by (2) and (3). The intersection of BL^1 and the boundary, BL^2 and the boundary are P^1 and P^2, respectively (see Fig.2(e)).

Step 5. Line up point P^1 and P^2, and make a palmprint coordinate system in which y-axis is line P^1P^2 and the original point is the midpoint of line segment P^1P^2 (see Figs.2(f) and 2(g)).

Step 6. Crop a sub-image with fixed size from the center of the image (see Fig.2(h)).

After preprocessing, the rotation and translation of the palmprints from the same palms are very little.

3 Feature Construction and Matching

Wavelet transform[17−19] is an effective tool for multiresolution feature extraction. Fig.3 shows the K-th level wavelet decomposition. In this figure, A_{k-1} is the approximation image of the $(K-1)$-th level decomposition and A_k, H_k, V_k, D_k are the approximation, horizontal, vertical and diagonal detail images of the K-th level decomposition, respectively. In this paper, the original image I is used as A_0. So after it is decomposed to the J-th level, the original image I is represented by $3J + 1$ sub-images:

$$[A_J, \{H_i, V_i, D_i\}_{i=1,\ldots,J}] \tag{7}$$

where A_J is a low-resolution approximation of original image, and H_i, V_i, D_i are the wavelet sub-images containing the image details in horizontal, vertical and diagonal directions at different scales (2^i). The amplitudes in H_i, V_i, D_i ($1 \leqslant i \leqslant J$) correspond to the horizontal high frequency (horizontal edges), vertical high frequency (vertical edges) and diagonal high frequency (diagonal edges), respectively. Fig.4 shows an example of the 2-level DWT decomposition of an image.

The wavelet energy in horizontal, vertical and diagonal directions at i-th level is, respectively, defined as:

$$E_i^h = \sum_{x=1}^{M}\sum_{y=1}^{N}(H_i(x,y))^2 \tag{8}$$

$$E_i^v = \sum_{x=1}^{M}\sum_{y=1}^{N}(V_i(x,y))^2 \tag{9}$$

$$E_i^d = \sum_{x=1}^{M}\sum_{y=1}^{N}(D_i(x,y))^2 \tag{10}$$

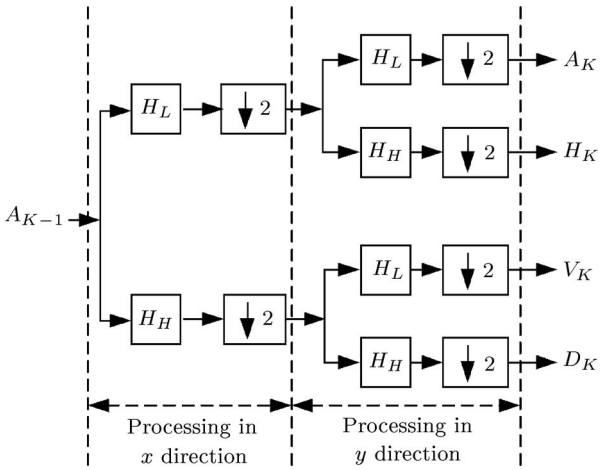

Fig.3. Two-dimensional DWT.

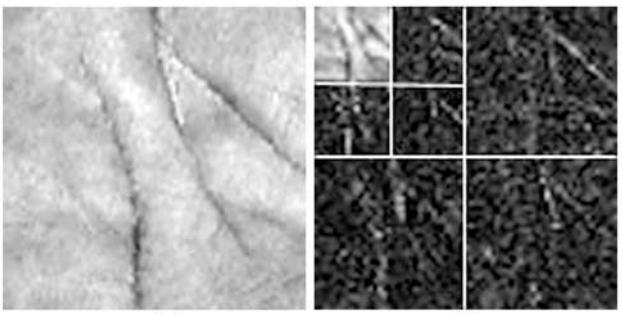

Fig.4. Example of 2-D DWT. (a) Original image. (b) Decomposed image.

These energies reflect the strength of the images' details in different direction at the i-th wavelet decompose level. The details of a palmprint are the principal lines, wrinkles and ridges. Hence, (8)–(10) can describe the intensity of these features in different orientation at the i-th wavelet decomposition level (scale). Because the amplitudes of wavelet coefficients of a nonoscillating pattern increase with the extension of wavelet decomposition scale while those of a high frequency oscillating pattern at large scales are much smaller than those at fine scale which matches the spatial frequency of the oscillations[18], the energy of principal lines and wrinkles, which are nonoscillating patterns, are concentrated at the large wavelet decomposition scales and the most energy of ridges, which are oscillating pattern, are focused at the small scales. So the feature vector,

$$(E_i^h, E_i^v, E_i^d)_{i=1,2,\ldots,M} \tag{11}$$

where M is the total wavelet decomposition level, can describe the global details information of a palmprint efficiently.

Obviously, the vectors computed from (8)–(11) are global features of a palmprint. These features extracted from the whole images fail to preserve the information concerning the spatial location of different details, so it cannot efficiently characterize palmprints. To deal with this problem, we can firstly divide the detail images into $S \times S$ non-overlap blocks equally (Fig.5), and then compute the energy of each block. After that, the energies of all blocks are used to construct a vector:

$$\begin{aligned}\boldsymbol{V} = &(V_{11}, V_{12}, \ldots, V_{1(3\times S\times S)}, \ldots, V_{M1},\\ &V_{M2}, \ldots, V_{M(3\times S\times S)})\end{aligned} \tag{12}$$

where M is the maximum level the image is decomposed to and V_{ij} $(j = 1, \ldots, 3\times S\times S)$ is the energies computed from the detail images of the i-th wavelet decomposition level.

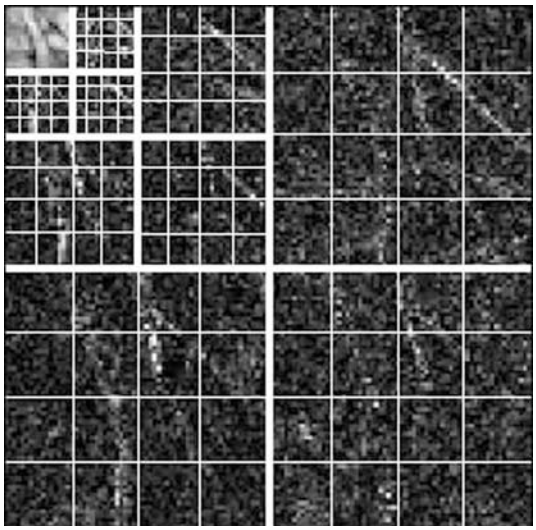

Fig.5. Division of the detail images at each scale.

Finally, the vector is normalized by the sum of $\boldsymbol{V}$. This normalized vector $\boldsymbol{V}$ is called the *wavelet energy feature* (*WEF*) and $\boldsymbol{V}^i = (V_{i1}, V_{i2}, \ldots, V_{i(3\times S\times S)})$ is called *the i-th level WEF*.

The complete process to compute WEF of a palmprint can be summarized as below:

1. Orientate the palmprint image;
2. Crop an $N \times N$ rectangular sub-image from the centre of the palm;
3. Decompose this sub-image to the J-th scale by a 2D-wavelet transform;
4. Divide each detail image into $S \times S$ non-overlapping blocks;
5. Compute the energy of each block and construct the feature vector;
6. Normalize this vector to form the WEF.

According to its construction, WEF $\boldsymbol{V}$ is composed of the different level WEFs, which have different abilities to discriminate palmprints. We use the following weighted cityblock distance to measure the similarity between two WEFs $\boldsymbol{V}_1$ and $\boldsymbol{V}_2$:

$$D(\boldsymbol{V}_1, \boldsymbol{V}_2) = \sum_{i=1}^{M} c_i \sum_{j=1}^{3\times S\times S} |\boldsymbol{V}_1^i(j) - \boldsymbol{V}_2^i(j)| \tag{13}$$

where M is the total wavelet decomposition level; $S \times S$ is the number of blocks that each detail image is divided; $\boldsymbol{V}_1^i = (V_1^i(1), V_1^i(2), \ldots, V_1^i(3 \times S \times S))$ and $\boldsymbol{V}_2^i = (V_2^i(1), V_2^i(2), \ldots, V_2^i(3 \times S \times S))$ are the i-th level WEF of $\boldsymbol{V}_1$ and $\boldsymbol{V}_2$; c_i is the weight for the i-th level WEF. We should decide c_i according to the discriminability of the i-th level WEF: the stronger the discriminability is, the larger the c_i is. If $c_i = 1$, (13) becomes the cityblock distance.

Given a palmprint database, the cityblock distances between the i-th level WEF of each sample and the i-th level WEF of the remaining samples can be computed. The distribution of distances generated from pairs of palmprints from the same palms is called the genuine distribution ($p_G(D)$) and from different palms is called the impostor distribution ($p_I(D)$). Fig.6 shows an example of these distributions. The overlapped area of $p_G(D)$ and $p_I(D)$ (the shadowed area in Fig.6) is called *minimum total error rate* (*MTER*), which can reflect the discriminability of the i-th level WEF: the smaller the MTER is, the stronger the discriminability is. MTER of the i-th level WEF can be obtained as follows:

$$R_i = \int_t^{\infty} p_G(D)\mathrm{d}D + \int_0^t p_I(D)\mathrm{d}D, \tag{14}$$

where t is the distance corresponding to the intersecting point of $p_G(D)$ and $p_I(D)$. Then we define the weight of the i-th level WEF c_i in this way:

$$c_i = \frac{1}{R_i \times \sum_{j=1}^{M} \frac{1}{R_j}}. \tag{15}$$

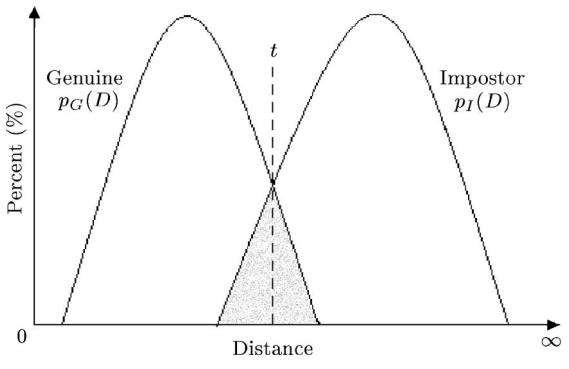

Fig.6. Example of genuine and impostor distributions.

Palmprint recognition involves a training stage and a recognition stage. In the training stage, WEFs of the

training samples are computed, and the template of a palm is obtained by averaging the WEFs of all training samples captured from the same palm and stored in a template database. In the recognition stage, WEF of the input palm is computed and then, by using weighted cityblock distance, this WEF is compared with the stored templates to obtain the recognition result.

4 Experimental Results and Comparisons

These experiments made use of a database of 3,200 palmprint images from 320 palms. These palmprints were taken from people of different ages and both sexes. Ten images were captured from each palm. Six of these were used to train the template and the remaining four samples were employed to test. The size of the original palmprint images was 384×284 pixels. The central 128×128 part of the image was cropped to represent the whole palmprint. Fig.7 shows some samples from our database. Using Harr wavelet, the images were decomposed to the 5th level. Each detail image is divided into 4×4 non-overlapping blocks. The weighted cityblock distance is used to measure the similarity between WEFs.

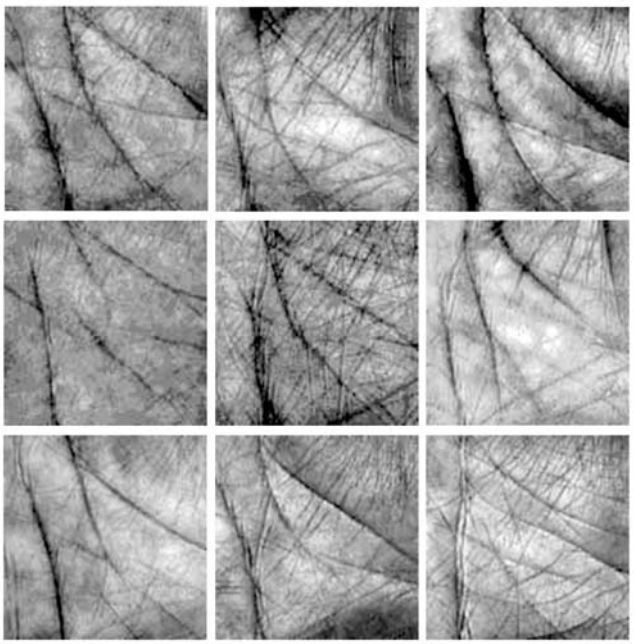

Fig.7. Some samples used in the experiments.

4.1 Parameters Selection

To use the weighted cityblock distance to measure the similarity between two WEFs, we should first select the parameter c_i for each level WEF. We use all of training samples to compute the weights. The genuine and impostor distribution of the 1st to 5th level WEF are plotted in Fig.8. The MTERs of these level WEFs are listed in Table 1. According to their MTERs, the order of the discriminabilities of these level WEFs, from strong to weak, is the 4th, 3rd, 5th, 2nd, and 1st levels. Using (15), the weights of these level WEFs can be easily obtained (see Table 1).

Table 1. MTERs and Weights of Each Wavelet Decomposition Level

Level	1st	2nd	3rd	4th	5th
MTER (R_i)	11.4	7.07	4.91	4.84	5.35
Weight (c_i)	0.11	0.17	0.25	0.25	0.23

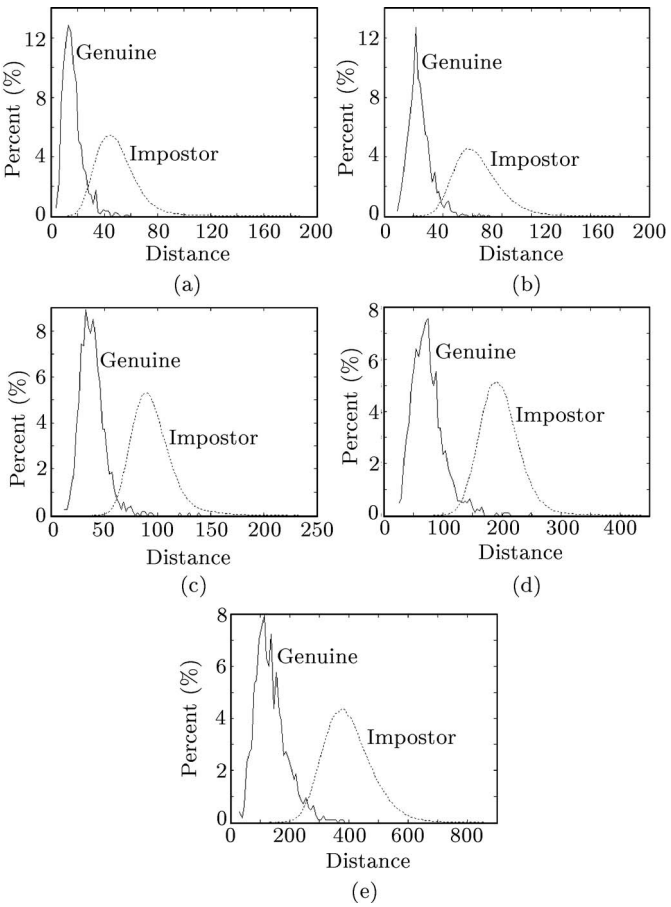

Fig.8. Genuine and impostor distributions of the 1st to 5th level WEF. (a) 1st level. (b) 2nd level. (c) 3rd level. (d) 4th level. (e) 5th level.

4.2 Rotation and Translation Test

Though the rotation and translation of the palmprints from the same palms are very little after preprocessing, it is impossible to remove all of them. To quantificationally investigate the robustness of the proposed approach to rotation and translation, 50 palmprints captured from different palms are selected randomly from our palmprint database. These images are translated and rotated using different distances and angles. Some of the testing palmprints and their rotated and translated versions are shown in Fig.9. Then, the translated and rotated palmprints are matched with the original ones by using our proposed approach. The average

matching distances are shown in Figs.10–11. For comparison, the average distance (66.9) among the palmprints captured from the same palm (average within-class distance), which is computed by using all of the samples in the palmprint database, is also plotted in these figures. According to Fig.10, when the rotational angle is between -4° and 4°, the average distances between the rotated and original palmprints are smaller than the average within-class distance. Therefore, our approach is robust when the rotational angle is within this range. From Fig.11, when the translational distance is within the range $[-4, 4]$ pixels, the approach is also robust.

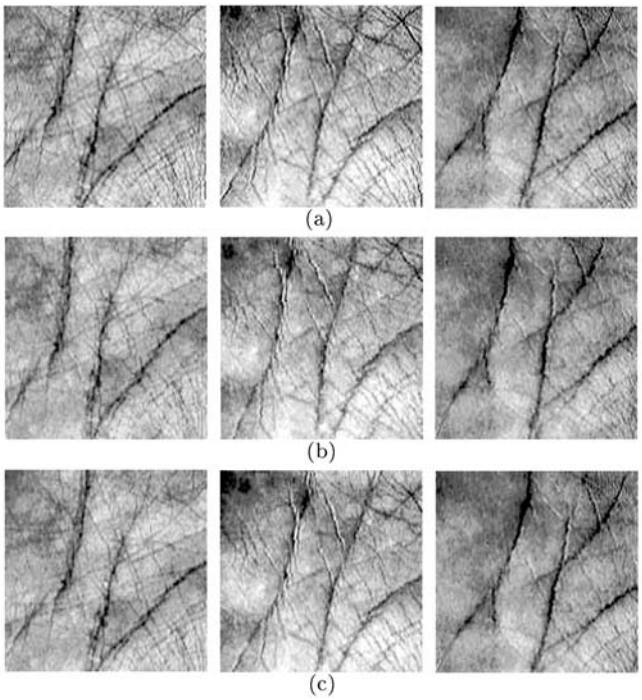

Fig.9. Some palmprints and the rotated and translated versions. (a) Original images. (b) Rotated images. (c) Translated images.

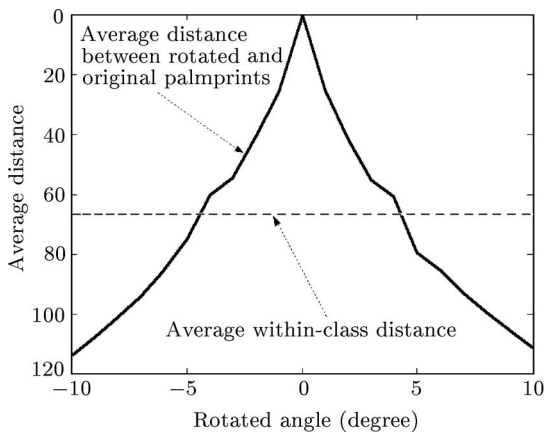

Fig.10. Average matching distances between the rotated and original palmprints.

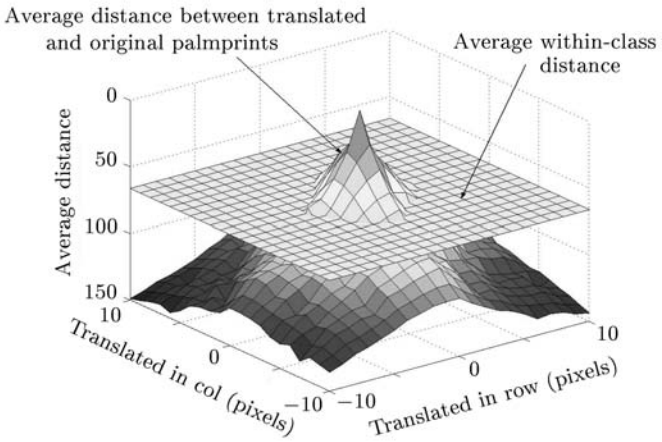

Fig.11. Average matching distances between the translated and original palmprints.

4.3 Palmprint Matching

To test the performance of the proposed approach in palmprint matching, the WEF of each testing sample is matched against each stored template. A total of 409,600 ($320 \times 4 \times 320$) matchings have been performed, in which 1,280 (320×4) matchings are genuine matchings. The genuine distribution and the impostor distribution are shown in Fig.12. It is shown that there are two distinct peaks in the distributions of the matching distances. One (located around 62) corresponds to the correct matching distance and another (located around 175) corresponds to the incorrect matching distance. These two peaks are widely separated and the overlapped area is very little (MTER is only 1.2%). Hence the proposed approach can clearly discriminate between palmprints.

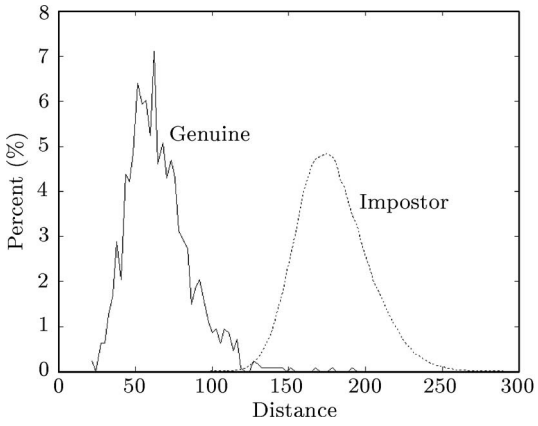

Fig.12. Distributions of correct and incorrect matching distances.

4.4 Palmprint Verification

Palmprint verification, also called one-to-one matching, involves answering the question "Whether this person is whom he claims to be" by examining his/her

palmprint. In palmprint verification, a user indicates his/her identity. Therefore, the WEF of the input palmprint is only matched against his/her stored template. To determine the accuracy of the verification, the WEF of each testing sample is matched against each stored template. If the matching distance does not exceed an appointed threshold, this testing palmprint is accepted. Otherwise, it is rejected. The performance of a verification method is often measured by the false accept rate (FAR) and false reject rate (FRR). We should try to make these two rates as low as possible. However, these two rates contradict each other and cannot be lowered at the same time, so depending on the application, a tradeoff is called for: for high security systems, such as some military systems, where security is primary criterion, the FAR should be reduced, while for low security systems, such as some civil systems, ease-of-use is also important, so the FRR should be reduced. To test the performance of a verification method with respect to this tradeoff, we usually plot the so-called *Receiver Operating Characteristic* (ROC) curve, which plots the FAR against the FRR. The ROC curves of the proposed approach are plotted in Fig.13. The equal error rate (EER, where FAR equals FRR) is 0.76%. This figure shows that the proposed approach has a good performance in palmprint verification.

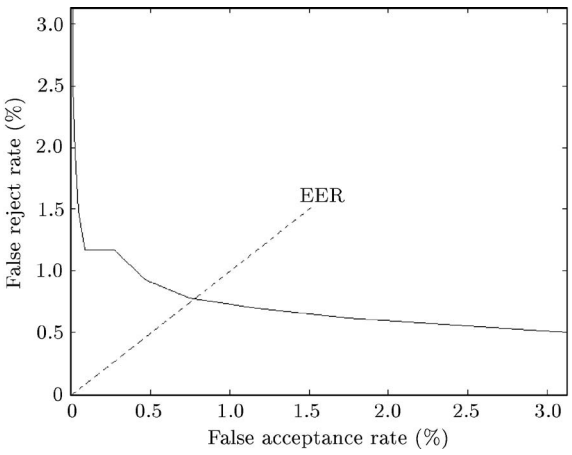

Fig.13. Receiver operating characteristic (ROC) curve of the proposed approach.

4.5 Palmprint Identification

Palmprint identification, also called one-to-many matching, is to answer the question "Who is this person?" according to his palmprint. To identify a person, the WEF of his/her palmprint has to be matched against all of the stored templates and the label of the most similar template is regarded as the identification result. In our one-to-320 matching, all of the 1,280 (320×4) testing images were used and 99.45% accuracy was obtained.

4.6 Comparisons with Other Palmprint Recognition Techniques

Our approach has been compared with Duta's method[13] and Li's algorithm[14]. In Duta's method, the lines of a palmprint were firstly extracted by directly binarizing the offline palmprint images (which were obtained by pressing an inked palm on a paper) with an interactively chosen threshold, and then some feature points and their orientation were extracted from these lines to verify the identity. Thirty 400×300 resolution offline images captured from three persons were used in their experiments. They reported 95% accuracy for their one-to-one matching test. It is evident that the recognition accuracies of this method are dependent heavily on the result of the line extraction. Because of the noise and unexpected disturbance such as the movement of hand, or variables in lighting or settings, the qualities of online palmprints (which are captured online by a CCD-camera-based device) are much worse than those of offline images. This makes it much more difficult to extract lines from online palmprint images. Up to now, there is no effective line extraction method for online palmprints yet. Therefore, we use Duta's reported experimental results here for comparison.

In Li's algorithm, the R features and θ features of the palmprint were extracted from the frequency domain to identify different persons. R features showed the intensity of the lines of a palmprint and θ features showed the direction of these lines. However, all of these features could not reflect the spatial position of these lines since they were extracted in the frequency domain. With the result that these features were not able to strongly discriminate between palmprints. Li's algorithm has been applied in our database and the accuracies in the one-to-one and one-to-320 matching are 96.32% and 94.53%, respectively.

Obviously, the results of the proposed approach are much better than those of Duta's and Li's. Table 2 summarizes and compares our approach with the methods of Duta and Li with respect to database size, image size, feature extraction, analysis method and accuracies.

Table 2. Comparison of Different Palmprint Recognition Techniques

Techniques	Duta's method[13]	Li's algorithm[14]	Our approach
Database size	30 images (from 3 palms)	3,200 images (from 320 palms)	3,200 images (from 320 palms)
Feature extraction	Feature points	R feature and θ feature	WEF
Analysis method	Single-resolution	Single-resolution	Multi-resolution
Image size	400×300	128×128	128×128
One-to-one matching accurate rates	95%	96.32%	99.24%
One-to-many matching accurate rates	Not presented	94.53% (One-to-320 matching)	99.45% (One-to-320 matching)

5 Conclusion and Future Work

Palmprint is a relative new biometric method to recognize a person. The basic features in a palmprint, including principal lines, wrinkles and ridges, have different resolutions. This observation motivates us to analyze the palmprint using multi-resolution analysis method. In this paper, a novel palmprint feature, named wavelet energy features (WEF), is defined by employing wavelets, which is a powerful tool of multi-resolution analysis. WEF can reflect the wavelet energy distribution of the principal lines, wrinkles and ridges in several directions at different wavelet decomposition levels (scale). The discriminability of each level WEF is also investigated and it shows that the order of these discriminabilities, from strong to weak, is the 4th, 3rd, 5th, 2nd, and 1st level. In palmprint matching, these different discriminabilities are used to define a weight for each level WEF to compute a weighted city block distance. It also shows that the proposed approach is robust to some extent in rotation and translation of the images. The experimental results demonstrate the effect of the proposed approach.

In recent years, some translation- and scale-invariant wavelet transform[20] have been proposed. In the future work, we will investigate these wavelet transform in palmprint recognition.

References

[1] Zhang D. Automated Biometrics — Technologies and Systems. Kluwer Academic Publishers, 2000.

[2] Jain A, Bolle R, Pankanti S. Biometrics: Personal Identification in Networked Society. Kluwer Academic Publishers, 1999.

[3] Jain A, Hong L, Bolle R. On-line fingerprint verification. *IEEE Trans. Pattern Analysis and Machine Intelligence*, 1997, 19(4): 302–313.

[4] Coetzee L, Botha E C. Fingerprint recognition in low quality images. *Pattern Recognition*, 1993, 26(10): 1441–1460.

[5] Wildes R P. Iris recognition: An emerging biometric technology. In *Proc. the IEEE*, 1997, 85(9): 1348–1363.

[6] Boles W W, Boashash B. A human identification technique using images of the iris and wavelet transform. *IEEE Trans. Signal Processing*, 1998, 46(4): 1185–1188.

[7] Liao P, Shen L. Unified probabilistic models for face recognition from a single example image per person. *Journal of Computer Science and Technology*, 2004, 19(3): 383–392.

[8] Gao Y, Leun M K H. Face recognition using line edge map. *IEEE Trans. Pattern Analysis and Machine Intelligence*, 2002, 24(6): 764–779.

[9] Campbell Jr J P. Speaker recognition: A tutorial. In *Proc. the IEEE*, 1997, 85(9): 1437–1462.

[10] Chen K. Towards better making a decision in speaker verification. *Pattern Recognition*, 2003, 36(2): 329–346.

[11] Jain A, Ross A, Prabhakar S. An introduction to biometric recognition. *IEEE Trans. Circuit and System for Video Technology*, 2004, 14(1): 4–20.

[12] Zhang D, Shu W. Two novel characteristics in palmprint verification: Datum point invariance and line feature matching. *Pattern Recognition*, 1999, 32: 691–702.

[13] Duta N, Jain A, Mardia K V. Matching of palmprint. *Pattern Recognition Letters*, 2001, 23(4): 477–485.

[14] Li W, Zhang D, Xu Z. Palmprint identification by Fourier transform. *International Journal of Pattern Recognition and Artificial Intelligence*, 2002, 16(4): 417–432.

[15] You J, Li W, Zhang D. Hierarchical palmprint identification via multiple feature extraction. *Pattern Recognition*, 2002, 35(4): 847–859.

[16] Han C, Chen H L *et al.* Personal authentication using palmprint features. *Pattern Recognition*, 2003, 36(2): 371–381.

[17] Mallat S, Zhong S. Characterization of signals from multiscale edges. *IEEE Trans. Pattern Analysis and Machine Intelligence*, 1992, 14(7): 710–732.

[18] Mallat S, Hwan W L. Singularity detection and processing with wavelets. *IEEE Trans. Information Theory*, 1992, 38(2): 617–643.

[19] Rioul O, Vetterli M. Wavelets and signal processing. *IEEE Signal Processing Magazine*, 1991, 8(4): 14–38.

[20] Xiong H, Zhang T. A translation- and scale-invariant adaptive wavelet transform. *IEEE Trans. Image Processing*, 2000, 9(12): 2100–2108.